Science Bulletin 64 (2019) 1325–1335

Contents lists available at ScienceDirect

Science Bulletin

journal homepage: www.elsevier.com/locate/scib

Article

Nature and evolution of the lithospheric mantle revealed by water contents and He-Ar isotopes of peridotite xenoliths from Changbaishan and Longgang basalts in Northeast China

Qinghu Xu [a,b], Jiaqi Liu [a,b,*], Huaiyu He [b,c,d], Yunhui Zhang [e]

[a] Key Laboratory of Cenozoic Geology and Environment, Institute of Geology and Geophysics, Chinese Academy of Sciences, Beijing 100029, China
[b] University of Chinese Academy of Sciences, Beijing 100049, China
[c] College of Earth Sciences, Chinese Academy of Sciences, Beijing 100029, China
[d] Key Laboratory of Earth and Planetary Physics, Institute of Geology and Geophysics, Chinese Academy of Sciences, Beijing 100029, China
[e] State Key Laboratory of Geohazard Prevention and Geoenvironment Protection, Chengdu University of Technology, Chengdu 610059, China

ARTICLE INFO

Article history:
Received 21 May 2019
Received in revised form 20 June 2019
Accepted 23 June 2019
Available online 6 July 2019

Keywords:
Subcontinental lithospheric mantle
Peridotite xenoliths
Mineral chemistry
He-Ar isotopes
Water contents
Northeast China

ABSTRACT

The nature and evolution of the lithospheric mantle underlying Northeast (NE) China were investigated by assessing the mineral chemistry, water contents, and noble gas (He-Ar) isotopes of peridotite xenoliths captured by Cenozoic basalts from the Changbaishan and Longgang regions. The xenoliths, which have 863–1141 °C equilibration temperatures, primarily comprise spinel lherzolites and rare spinel harzburgites. The $Mg^{\#}$ (Fo) values of olivine in the peridotite xenoliths vary from 86.9 to 91.3. The clinopyroxenes have high Ti/Eu and low $(La/Yb)_N$, and their chondrite-normalized rare earth elements (REEs) exhibit light REE-depletion to -enrichment patterns, indicating that the mantle underneath the investigated region was predominantly subjected to partial melting (1%–10%) and was metasomatized by silicate melts. The measured $^{3}He/^{4}He$ ratios of the Changbaishan xenoliths have a narrow range from 5.8 Ra to 8.4 Ra with an average of 7.4 Ra. The $^{3}He/^{4}He$ isotopic ratios of the Longgang xenoliths varied from 4.7 Ra to 8.1 Ra with an average of 5.9 Ra; slightly lower than the Changbaishan xenoliths. The whole-rock H_2O contents of the studied peridotite ranged from 9 to 132 ppm. The high H_2O contents in excess of 50 ppm (up to 132 ppm) might represent newly accreted and cooled asthenospheric materials, while those with H_2O contents lower than 50 ppm (as little as 9 ppm) may represent thinned, relic, ancient lithospheric mantle. These geochemical evidences, in combination with published data, indicated that the lithospheric mantle beneath the Changbaishan and Longgang in NE China is dominated by the younger and more fertile lithospheric mantle with a minor ancient and refractory keel. In addition, the lithospheric mantle of this area was metasomatized by melts related to the recent subduction event (e.g., Pacific oceanic plate). Therefore, the westward-dipping Pacific oceanic plate subduction had an important contribution to the transformation of the lithospheric mantle beneath NE China.

1. Introduction

The subcontinental lithospheric mantle (SCLM) of eastern China, located in the easternmost part of the North China Craton, underwent a transformation from a cold, refractory, Archean cratonic mantle ranging ca. from 150 to 220 km in thickness to a hot, fertile, Phanerozoic non-cratonic lithospheric mantle ranging ca. 60–120 km in thickness [1–3]. Moreover, previous studies have proved that this transformation was associated with significant Phanerozoic Pacific subduction [4–6]. Eastern China thus constitutes a suitable natural study site for deciphering how the transformation of the continental lithosphere occurred under the setting of a subduction environment.

Peridotite xenoliths captured by alkali volcanic basalts can directly be used to study the nature and evolution of the SCLM because their geochemical signatures are typically well conserved due to the rapid upwelling and “quench” effect of rapid surface cooling [7]. Numerous studies over the past few decades have investigated Northeast (NE) China mantle xenoliths to explain the nature and evolution of the SLCM [8–12]. Previous research that constrains the nature of the mantle lithosphere beneath NE China was mainly based on the major elements, trace elements, and Sr–Nd–Hf–Li isotopic compositions of the mantle xenoliths

* Corresponding author.
E-mail address: jiaqiliu@mail.iggcas.ac.cn (J. Liu).

https://doi.org/10.1016/j.scib.2019.07.006
2095-9273/

[13–17]. Although almost all previous studies indicate that the refractory subcontinental keel beneath NE China was mostly replaced by a younger and fertile lithospheric mantle during the Cenozoic, there are still some problems that need to be clearly addressed. For example, a previous study indicated that the harzburgites from Longgang, NE China, are products of the lithosphere mantle interaction with asthenosphere-derived melts during lithospheric thinning. A study of the oxidation state of the lithospheric mantle between NE China (e.g., Kuandian, Longgang, Changbaishan) indicates that the studied metasomatized peridotites have fO_2 values ranging from FMQ–1.32 to +0.39, which are similar to the samples free of metasomatism [16]. This study argued that the lithospheric mantle beneath this area was also metasomatized by asthenosphere-derived basaltic melts. Recently, a very fascinating study of Longgang spinel-facies peridotite xenoliths was carried out by Lin et al. [17]. In this study, Longgang spinel-facies peridotite xenoliths could be divided into two groups according to their detailed petrography and whole-rock and mineral compositions. The group two fertile peridotites without spinel-pyroxene intergrowths show evidence for metasomatism by melts similar to the Cenozoic basalts at high melt–rock ratios, whereas the group one moderately refractory peridotites with ubiquitous spinel-pyroxene intergrowths only show evidence for metasomatism by residual melts at low melt-rock ratios. However, the study of the lithospheric mantle beneath the Changbaishan area suggests that the lithosphere mantle was metasomatized by subduction-related, fluid-bearing silicate melts, rather that the asthenosphere-derived basaltic melts [18]. The isotope study of Li suggests that the lithospheric mantle beneath the Longgang area has been not only modified by melts derived from the subducted Pacific plate but also refertilized by melts from the underlying asthenosphere [15]. Thus, the nature of the metasomatic agent of the lithosphere mantle beneath NE China is still unclear.

In this study, we conducted an integrated analysis of the mineral chemistry, H_2O contents, and He-Ar isotopes within peridotite xenoliths from Changbaishan and Longgang in NE China. Our objectives were: (1) to assess the distribution of He-Ar isotopes and H_2O contents in the peridotite xenoliths and evaluate the mechanisms controlling H_2O content; (2) to discuss the partial melting and metasomatism of the lithospheric mantle, and (3) to provide additional information relating to the metasomatic agent and the nature and evolution of the SCLM underlying the Changbaishan and Longgang, NE China.

2. Geological setting and petrography

The earliest North China Craton (NCC) crust formed at about 3.8 Ga and is considered to be among the most ancient Archean cratons [19]. It experienced multiple Late Archean and Paleoproterozoic tectonic stages [20–22]. Since the Phanerozoic, collision has occurred between the NCC and adjacent blocks and plates, following which different oceanic plates were subducted under the NCC [23–26]. These Late Paleozoic to Cenozoic subductions and collisions resulted in significant lithospheric mantle modification under the NCC [27–30].

The Changbaishan and Longgang regions lie on NE China (Fig. S1 online) and tectonically belong to the NE NCC. The NE NCC basement comprises Archean tonalite–trondhjemite–granodiorite (TTG) gneisses, granitoids, plus supracrustal rocks. The basement is covered by Proterozoic–Paleozoic strata, which contain metasedimentary and clastic sedimentary rocks, bimodal volcanic rocks, and thick carbonate deposits. Late Triassic–Early Jurassic and Early Cretaceous granitic rocks are significantly exposed on the NE NCC. Secular Kula and Pacific plate subduction caused calc-alkaline volcanism during the Late Cretaceous, which primarily contributed to the formation of the Changbaishan and Longgang volcanic fields. During the Miocene to Pliocene, minor eruptions of basaltic magmas occurred at a few scattered volcanoes in the Changbaishan volcanic field, while the Tianchi volcano was the main source of the basaltic magmas that erupted during the Early Pleistocene [31,32]. The Longgang volcanic field erupted only basaltic magmas during the Quaternary, with the last eruption occurring ca. 1600 years ago [33].

Significant peridotite and pyroxenite xenoliths have been documented from these Cenozoic alkali basalts. In this study, 22 peridotite xenoliths were sampled from the Changbaishan and Longgang volcanic fields. They are angular to round with diameters of 2–8 cm and can mainly be classified on modal mineralogy into lherzolites and harzburgites. The peridotite xenoliths possess protogranular textures and the mineral grains meet at well-developed triple junctions (Fig. S2 online). Some spinels exhibit a distinct sieve texture at the rim (Fig. S2d online). Twelve peridotites from the Changbaishan volcanic field were transported to the surface at ca. 19.9–2.6 Ma [34], all of which are lherzolites (Fig. S3 online). Ten peridotites from the Longgang volcanic field were sampled in volcanos aged at ca. 0.68–0.05 Ma [33], including eight lherzolites and two harzburgites. The lherzolites contain 55%–78% olivine, 9%–29% orthopyroxene, 5%–22% clinopyroxene, and 0.5%–3% spinel, while the harzburgites are composed of 70%–78% olivine, 18.5%–26% orthopyroxene, 3% clinopyroxene, and 0.5%–1% spinel. Modal proportions of minerals in the samples were estimated by spot counting more than 1000 grains.

3. Analytical methods

Analyses of the mineral chemistry were performed on olivines (ol), orthopyroxenes (opx), clinopyroxenes (cpx), and spinels (sp). Fresh crystals (ol, opx, cpx and sp) were picked out for the He-Ar isotopic analyses following the vacuum crushing method [35]. The *in-situ* analyses of mineral water contents were conducted by Fourier Transform Infrared Spectrometry (FTIR), following the unpolarized method of Kovács et al. [36]. Further information relating to the experimental procedures and data is provided in Supplementary material (online), respectively. The modal mineralogy and equilibration temperature results are listed in Table S1 (online), while those for mineral chemistry are listed in Tables S2 and S3 (online). Water contents and results for He-Ar isotopes are presented in Tables S4 and S5 (online), respectively.

4. Results

4.1. Xenolith mineral chemistry

The compositions of the spinel with sieve textures differ from the core to the rim, and we chose to use the data from the core. As for the other minerals, they are homogenous from the core to the rim, and thus we took the average compositions of the minerals.

4.1.1. Olivine and orthopyroxene

Olivines in the Changbaishan and Longgang xenoliths have $Mg^{\#}$ [$=100 \times$ molar $Mg/(Mg + Fe)$] values spanning a wide range of 86.9–91.3. The olivines possess comparable contents of CaO, NiO, and MnO of 0.00 wt%–0.20 wt%, 0.31 wt%–0.42 wt%, and 0.11 wt%–0.16 wt%, respectively.

The olivine $Mg^{\#}$ versus CaO plot demonstrates that the studied peridotite xenoliths primarily lie in the same field as the sub-Shanwang area fertile lithospheric mantle (Fig. 1a). The orthopyroxene $Mg^{\#}$ and $Cr^{\#}$ [$Cr^{\#} = 100 \times$ molar $Cr/(Cr + Al)$] values range

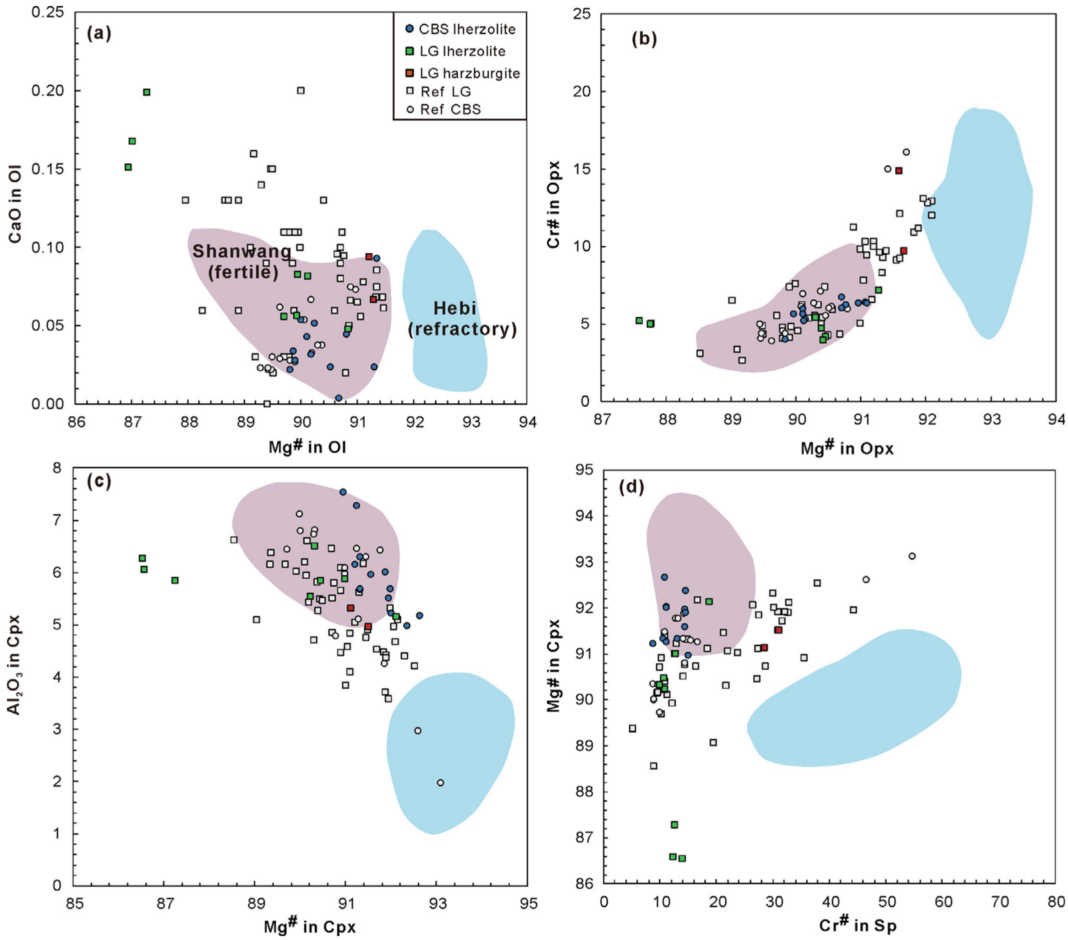

Fig. 1. Diagrams of mineral chemistry from Changbaishan and Longgang peridotite. (a) Olivine Mg# versus CaO, (b) orthopyroxene Mg# versus Cr#, (c) clinopyroxene Mg# versus Al_2O_3, and (d) spinel Cr# versus clinopyroxene Mg# in Changbaishan and Longgang peridotite xenoliths. The compositional fields of Shanwang and Hebi peridotite xenoliths are drawn according to Zheng et al. [37] and Zheng et al. [38]. Ref refers to peridotite xenoliths from Changbanshan and Longgang in previous studies [16–18].

from 87.6 to 91.7 and 4.0 to 14.9, respectively, and exhibit a positive correlation (Fig. 1b).

4.1.2. Clinopyroxene

All the clinopyroxenes from the Changbaishan and Longgang peridotite xenoliths are Cr-diopside with Cr_2O_3 contents of 0.53 wt%–1.23 wt%. They have Mg# and Cr# values of 86.5–92.6 and 5.7–13.6, respectively. The Al_2O_3 contents and Mg# values of the clinopyroxenes are negatively correlated, and all the samples grouped into the field associated with the sub-Shanwang area fertile lithospheric mantle (Fig. 1c).

The clinopyroxenes have between 11.8 and 32.5 ppm total rare earth elements (REE) and $(La/Yb)_N$ values ranging from 0.04 to 1.76 ("*N*" indicates chondrite normalized values). The analyzed clinopyroxenes exhibit diverse patterns of chondrite-normalized REEs (Fig. 2). Based on the different REE patterns in the clinopyroxene, the studied peridotite could be subdivided into three groups: (1) LREE-depleted Group 1; (2) Group 2, which display spoon-shaped and nearly flat REE patterns; and (3) Group 3, which exhibit convex-upward patterns, with a peak at Eu. Interestingly, the heavy rare earth element (HREE) distributions of the majority of the clinopyroxenes from the Changbaishan and Longgang peridotite xenoliths were relatively flat. When normalized to the primitive mantle, most of the clinopyroxenes demonstrated negative Ba, Nb, Ta, Zr, Hf, and Ti anomalies and positive U, Th, and Pb anomalies (Fig. 2).

4.1.3. Spinel

The compositions of the spinels in the studied peridotites varied widely considering the Mg# values (67.5–80.0), Cr_2O_3 contents (8.32 wt%–27.45 wt%), and Cr# (8.8–31.0). The Cr# values and the Mg# values of coexisting clinopyroxenes are within the region of the fertile lithospheric mantle from Shanwang (Fig. 1d). Furthermore, the olivine and spinel compositions of the Changbaishan and Longgang peridotite xenoliths are akin to those of the abyssal peridotites but tend toward compositions with greater fertility (Fig. 3). The highly variable concentrations of Cr_2O_3 (8.32%–27.45%), and thus the Cr# values (8.8–31.0), of the spinels can probably be attributed to metasomatic processes.

4.2. Equilibration temperatures

As the use of a single geothermometer can result in systematic errors, temperatures recorded using several geothermometers are more convincing. We thus robustly calculated the equilibration temperatures using Ca-in-orthopyroxene (T/BK) [44], Na-in-ortho pyroxene-clinopyroxene (T/W) [45], and clinopyroxene-spinel (T/SS) thermometers [46]. Previous analyses reported that the pressures for the stable occurrence of Cr-spinel in peridotite range between 8 and 25 kbar [47,48]. Hence, temperatures were calculated under the condition of 15 kbar. The estimated temperatures were thus 863–1,055 °C by T/W, 885–1,141 °C by T/BK, and 900–1,062 °C by T/SS, and exhibited high consistency. The harzburgites were associated with comparatively higher calculated

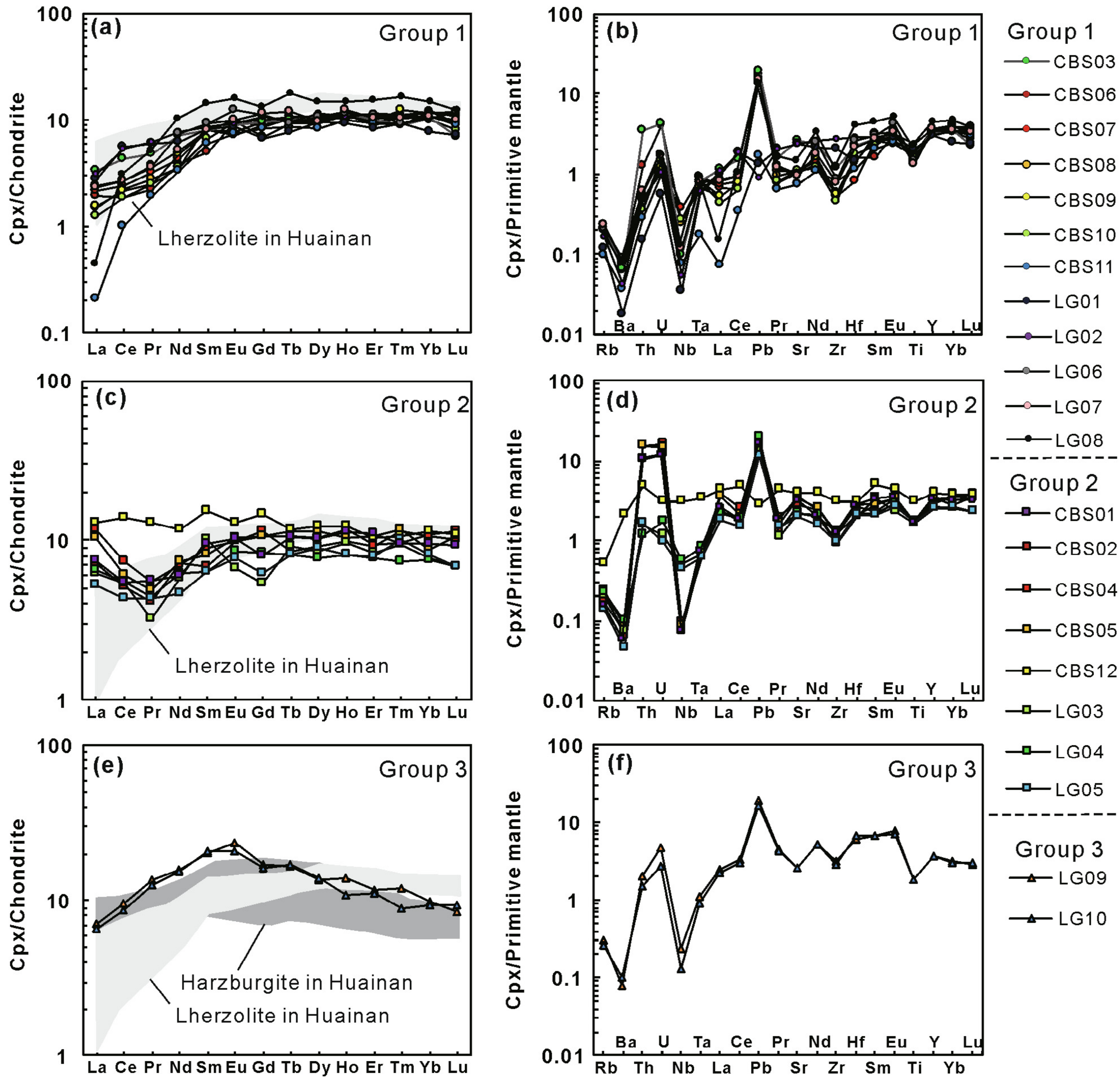

Fig. 2. REE (chondrite-normalized) (a, c, e) and trace element (primitive mantle-normalized) (b, d, f) compositions of clinopyroxenes in Changbaishan and Longgang peridotite xenoliths. Values for the chondrite are from Sun and McDonough [39] and for the primitive mantle are from McDonough and Sun [40]. The grey fields of Longgang samples are from Xu et al. [13].

temperatures than the lherzolites. The higher temperatures probably suggested a deeper origin or thermal perturbation by metasomatism.

4.3. H_2O content and hydrogen speciation

We have provided representative clinopyroxene and orthopyroxene infrared spectra in Fig. S4a, b (online). The IR OH absorption bands of clinopyroxene and orthopyroxene were categorized into the following groups: 3,630–3,620, 3,540–3,520, and 3,470–3,460 cm^{-1} for clinopyroxene, and 3,590–3,570, 3,525–3,515, and 3,425–3,415 cm^{-1} for orthopyroxene. These absorption bands exhibited comparable characteristics to those seen in previous studies and were thus attributed to structural OH vibration [49–52]. Analyses of hydrogen profiles were conducted on the relatively large clinopyroxene and orthopyroxene grains. No observable variations in the height, peak positions, and bandwidths of the absorption bands in the spectra collected in the core and rim regions were observed (Fig. S4c, d online).

H_2O contents were measured in the clinopyroxene (34–306 ppm) and orthopyroxene (15 to 120 ppm). The water contents of the minerals plus their modal proportions were combined to estimate whole-rock values for H_2O content ranging from 9 to 132 ppm, similar to the source of the mid-ocean ridge basalt (MORB, 50–200 ppm) [53,54] and previous research (Fig. 6). However they were substantially lower than estimations for the Ocean Island basalts (OIB), which are 300–1,000 ppm [55,56].

4.4. He-Ar isotopic compositions

4.4.1. Helium

The helium abundances of the Changbaishan and Longgang xenoliths varied widely (Supplementary data, online), ranging from 1.2×10^{-9} to 48.5×10^{-9} ccSTP/g in clinopyroxene,

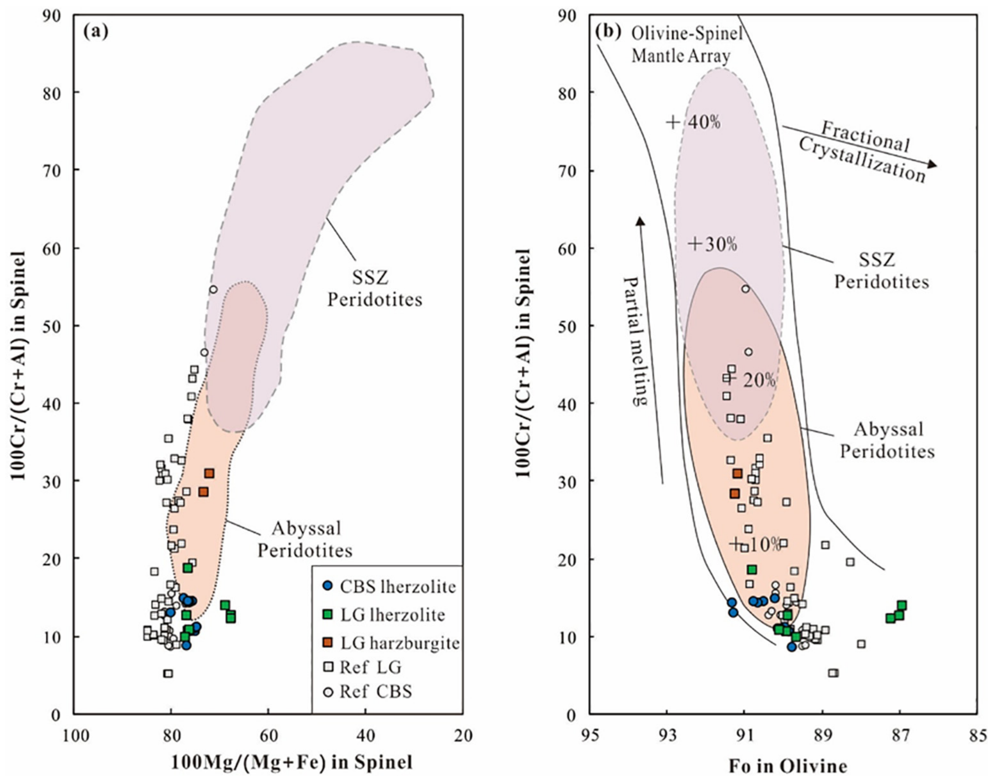

Fig. 3. Spinel Cr# versus spinel Mg# (a), Fo (b) contents in the coexisting olivines. The olivine-spinel mantle array and melting trend values are from Arai [41]. Data on the supra-subduction zone and abyssal peridotites are sourced from Pearce et al. [42] and Ishii et al. [43]. Data sources are consistent with Fig. 1.

0.1×10^{-9} to 13.4×10^{-9} ccSTP/g in olivine, 3.7×10^{-9} to 59.3×10^{-9} ccSTP/g in orthopyroxene, and 70.6×10^{-9} to 183.4×10^{-9} ccSTP/g in spinel. The measured $^{3}He/^{4}He$ ratios of the Changbaishan xenoliths have a narrow range from 5.8 Ra to 8.4 Ra with an average of 7.4 Ra. Most of the data were plotted within the error of the MORB range (Fig. S5a online). In contrast, the $^{3}He/^{4}He$ isotopic ratios of the Longgang xenoliths ranged from 4.7 Ra to 8.1 Ra with an average of 5.9 Ra, which is slightly lower than the Changbaishan xenoliths (Fig. S5c online). However, no systematic differences were detected in $^{3}He/^{4}He$ among the cogenetic minerals for both the Changbaishan and Longgang xenoliths.

4.4.2. Argon

The $^{40}Ar/^{36}Ar$ ratios within both Changbaishan and Longgang xenoliths ranged from 373 to 3196, which is significantly below the values typically found in continental xenoliths and the mantle source of MORB glasses [57–59]. The $^{40}Ar/^{36}Ar$ ratios are low either because of shallow-level contamination of atmospheric Ar or subduction-induced addition of air-derived Ar into the mantle [60]. Most samples from both the Changbaishan and Longgang xenoliths possessed low $^{4}He/^{40}Ar^{*}$ ($^{40}Ar^{*}$ is corrected for atmospheric Ar as $^{40}Ar^{*} = [^{36}Ar]_{\text{measured}} \times \{(^{40}Ar/^{36}Ar)_{\text{measured}} - (^{40}Ar/^{36}Ar)_{\text{AIR}}\}$) ratios (Fig. S5b, d online). Our He-Ar isotope compositions are consistent with previous studies (Fig. S5 online).

5. Discussion

5.1. Mantle xenolith petrogenesis

5.1.1. Peridotite melting history

Clinopyroxene Mg# values were negatively correlated with clinopyroxene Al_2O_3 contents (Fig. 1c) and positively correlated with spinel Cr# values (Fig. 1d), indicating the impact of partial melting. The compositional association between spinel Cr# and olivine Fo values can be used to quantify melt extraction from mantle rocks [61]. We thus deduced that after ≤10% partial melting, the Longgang and Changbaishan lherzolites constitute residues, whereas the Longgang harzburgites constitute residues after ~15% partial melting (Fig. 3b).

The moderately incompatible HREE concentrations in the clinopyroxene are generally only slightly impacted by later metasomatic activities. Research has indicated that trace elements in clinopyroxene such as Y and Yb can also provide an estimate of the degree of mantle peridotite partial melting [62,63]. The estimates suggest that lherzolites and harzburgites would be produced by 1%–6% fractional melting or 1%–10% batch melting (Fig. 4). As shown in Fig. 4, the two harzburgites display partial melting degrees similar to lherzolites, which is in contrast with the common petrological observations. Due to decompression, the garnet can transform, from the garnet phase to the spinel phase, into clinopyroxene plus spinel [64,65]. Secondary clinopyroxene may inherit the high HREE content in its parental garnet, which caused the harzburgites to fall close to most lherzolites in Fig. 4. We can use another formulation to calculate the degree of partial melting (F). The equation is the spinel $Cr^{\#}$:$F = 10\ln(Cr^{\#}) + 24$ [61]. From this, we can see that lherzolites and harzburgites produce 1%–7% and 11%–12% partial melting, respectively. As for the harzburgites, the results calculated by Cr# are more reliable.

5.1.2. Mantle metasomatism

Following partial melting, subsequent mantle metasomatism may modify the SCLM. The REE patterns of clinopyroxenes are variably enriched and cannot be solely attributed to partial melting (Fig. 2). Meanwhile, the deviation from the curve of partial melting suggests varying degrees of mantle metasomatism (Fig. 4). Mantle metasomatism comes in three basic varieties [66]: modal (introduction of obviously new phases such as amphibole and

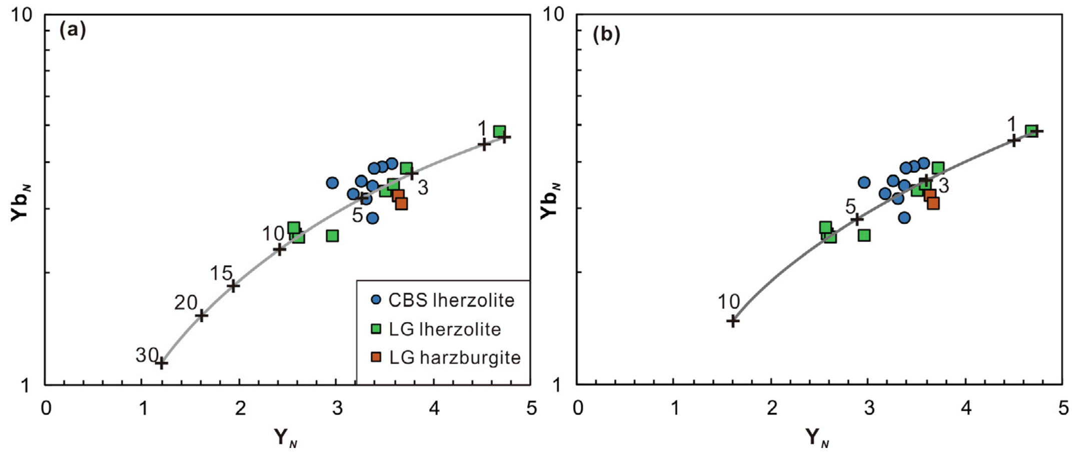

Fig. 4. Fractional partial melting modeling based on clinopyroxene compositions for the Changbaishan and Longgang peridotite (normalized to primitive mantle after McDonough and Sun [40]) (a) Batch melting; (b) fractional melting.

phlogopite); stealth (introduction of "primary" phases such as garnet and clinopyroxene), and cryptic (changes in elemental and isotopic composition of pre-existing minerals). The lack of modal metasomatic minerals such as amphibole, mica, or apatite (Fig. S2 online) indicates that the studied peridotite probably experienced cryptic metasomatism.

5.1.3. Nature of the metasomatic agents

Metasomatic agents that may affect the lithospheric mantle typically include fluids or hydrous silicate melts [67], CO_2-H_2O rich fluids [68], and carbonatite melts [69]. Metasomatism related to silicates and to carbonatites can be differentiated with the help of a $(La/Yb)_N$ versus Ti/Eu plot for clinopyroxenes [70]. The clinopyroxenes of the Changbaishan and Longgang peridotites possessed a wide Ti/Eu range as well as $(La/Yb)_N$ ratios that were moderate to low, which suggests that the evaluated peridotite might have experienced silicate metasomatism (Fig. 5). Thus, the metasomatic agents were aqueous fluids or hydrous silicate melts rather than carbonated melts [13,17,18].

The Changbaishan xenoliths have overall MORB-like $^3He/^4He$ ratios, although a few samples with the lowest He abundances displayed a lower $^3He/^4He$ trend (Fig. S5a online). As the in-vacuum crushing method preferentially releases fluid inclusion-trapped

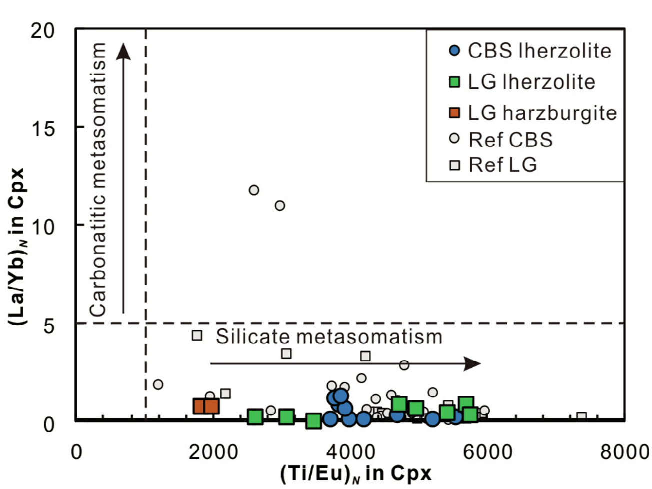

Fig. 5. Clinopyroxene $(La/Yb)_N$ versus $(Ti/Eu)_N$ for Changbaishan and Longgang peridotite. $(La/Yb)_N$ values are chondrite-normalized after Sun and McDonough [39]. Data sources are consistent with Fig. 4. Modified from Coltorti et al. [70].

noble gases, cosmogenic-derived ^3He and ^4He produced *in-situ* in the mineral matrix can be avoided to a large extent [71]. In addition, the young eruption age of the Cenozoic alkali basalts hosting the xenoliths suggests that the post-eruptive accumulation of both ^3He and ^4He is limited. The consistent $^3He/^4He$ (~6 Ra) in the Longgang xenoliths irrespective of their He contents also suggests that post-modifications on He isotopes are trivial. Thus, the He results of the xenoliths primarily represent the characteristics of the mantle source from which they originated.

The asthenospheric mantle source has relatively consistent $^3He/^4He$ ratios of 8 ± 1 Ra, as indicated by the global MORBs [72]. Compared with the $^3He/^4He$ ratios of typical MORBs, the slightly low $^3He/^4He$ ratios (7.4 and 5.9 Ra) of the Changbaishan and Longgang xenoliths suggests that the SCLM underneath the studied area has been refertilized by silicate melts/fluids. Previous He-Ar studies of xenoliths and megacrysts from the Changle area in Shandong Province demonstrate that the juvenile lithospheric mantle was again metasomatized by oceanic crust-derived melts, which resulted in the lowering $^3He/^4He$ of the clinopyroxene in the lherzolites and wehrlites [73]. Furthermore, different noble gas isotopic characteristics in peridotite xenoliths from eastern China indicate comprehensive refertilization of the lithospheric mantle by melt derived from oceanic crust [35]. Also, the observed $^4He/^{40}Ar^*$ in both the Changbaishan and Longgang xenoliths from the typical mantle production value (ca. 1–5) [57,74] to very low value of ca. 0.02 could be a mixture between major metasomatic fluids and minor SCLM relics, combined with the $^3He/^4He$ data. Therefore, the noble isotope geochemistry indicated that the mantle lithosphere beneath the Changbaishan and Longgang area was refertilized by subduction-related crustal components.

It is commonly accepted that SCLM usually has $^3He/^4He$ ratios of 5–7 Ra, such as the SCLM in Europe [75,76]. However, if the SCLM is metasomatized by silicate melts/fluids from an ancient subduction event, it will generate relatively low $^3He/^4He$ ratios. This is because that silicate melts/fluids from recycled components, such as a possible U and Th-rich material and will generate ^4He due to the decay of U-Th. For example, ancient recycled crustal materials, which are the enriched component in the mantle source of Pitcairn lavas, should generate ^4He by U and Th decay over time, and this would develop the mantle beneath this area with relatively low $^3He/^4He$ (0.1 Ra) [77]. Thus, we suggest that the mantle lithosphere beneath the Changbaishan and Longgang area was refertilized by the silicate melts/fluids, which mostly likely originated from the recent subduction event. The $^{40}Ar/^{36}Ar$ ratios of the xenoliths, approaching that of the air, support that they were metasomatized by fluid agents released by a recent young oceanic subducted slab if the shallow atmospheric contamination could be expelled [60], as peridotite xenoliths formed by the subduction of ancient continents mostly present relatively high $^{40}Ar/^{36}Ar$ ratios. Similar low $^{40}Ar/^{36}Ar$ of xenoliths from eastern China were reported by Su et al. [73] and were explained to be related to a recent subduction event.

Earlier research indicates that NE China experienced two dual subduction episodes during Mesozoic times, including the southward Paleo-Asian oceanic plate subduction during the Jurassic and the westward Pacific plate subduction since the Cretaceous [78]. Considering that the Late Cenozoic basalts in NE China (for example, the basalts in Songliao Basin) have higher water contents, which are related to the role (e.g., dehydration) of the subducted Pacific slab in the mantle transition zone [79,80], we therefore proposed that the mantle lithosphere beneath the studied area was refertilized by the silicate melts/fluids, which originated from the recent stagnant Pacific subduction. Our study (particularly our noble isotope results) indicates that the metasomatic agent was the silicate melts/fluids, which is related to the stagnant Pacific in the mantle transition zone. This conclusion is consistent with previous published research results [15,18]. However, we cannot rule out that the asthenospheric mantle-derived melts have some impact on the lithosphere transformation in this area, as argued by previous studies [13,15–17]. Thus, further study is needed to evaluate this fully.

5.2. Preservation and controlling factor of the initial mantle source H_2O content

The solubility of hydrogen in nominally anhydrous minerals (NAMs) rises as pressure increases at pressures below 3.5 GPa [81,82]. The first paper that reported on the water content in Chinese peridotites by FTIR in *Chem Geol* was by Yang et al. [83]. During the entrainment of peridotite xenoliths by host basalts, hydrogen in NAMs may be lost by decompression-induced diffusion. Simulation experiments have revealed that hydrogen contents in millimeter-size grains of NAMs will be thoroughly adjusted to changing conditions within several tens of hours [84,85]. However, large amounts of studies on peridotite xenoliths indicated that the original mineral H_2O contents in minerals, especially pyroxenes, can generally be preserved [51,86–89]. The inconsistency between experimental results and natural observations could be explained by the following factors: (1) hydrogen preservation in NAMs is controlled by the different ambient conditions, e.g., the H_2O contents of coexisting exotic melts as well as oxygen fugacities in the systems; (2) the experiments were mostly performed under water saturation, which is a rare occurrence in the mantle; (3) the experiment conducted by Kohlstedt and Mackwell [90] suggested that hydrogen percolation and preservation in NAMs are intimately related to the concentrations and diffusive rates of point defects; and due to the variability in diffusion rates, hydrogen losses in olivine typically occur alongside hydrogen retention in pyroxene from peridotite xenoliths [87,91,92].

Previous research on natural samples generally indicates better preservation of mantle-derived H_2O content in pyroxenes than in olivines [51,87,89,92]. We infer from the following evidence that peridotite xenolith pyroxenes in the Changbaishan and Longgang regions should have preserved their original H_2O contents: (1) the profile analyses reveal no observable core-to-rim H_2O content variations in the pyroxene grains (Fig. S4c, d online). Conversely, the typical OH distribution pattern as a result of water loss was higher in the core than the rim [91–93]; and (2) the clinopyroxene-orthopyroxene water partition coefficient (water content in clinopyroxene/orthopyroxene = 2.2) for the Changbaishan and Longgang peridotite was similar to that commonly reported for peridotite xenoliths found elsewhere [94]. In particular, it corroborates the peridotite xenoliths entrained by Cenozoic NCC basalts (2.2 ± 0.5 averaged from 150 samples) [89].

During mantle melting and magma fractionation, H_2O acts as an incompatible species with a partition coefficient similar to Ce [95,96]. When the H_2O content in pyroxene is chiefly controlled by partial melting, the H_2O contents would have a negative association with the $Mg^{\#}$ values in olivine [97]. As discussed above, the Changbaishan and Longgang peridotite was metasomatized by the silicate melt after basaltic melt extraction. The clinopyroxene and orthopyroxene H_2O contents are not correlated to the olivine $Mg^{\#}$ values (Fig. 6b, c), suggesting that the large H_2O content variation among different samples cannot be fundamentally attributed to partial melting. Furthermore, a lack of linear correlation between whole-rock H_2O and $(La/Yb)_N$ also demonstrates that mantle metasomatism did not control the H_2O contents of the peridotite (Fig. 6d) [99]. We propose that the significant H_2O-content variation in the lithospheric mantle beneath Changbaishan and Longgang thus cannot only be ascribed to partial melting and mantle metasomatism. The large variation in H_2O contents of the studied peridotite may reflect the features of their source and correspond to the complex evolution of the lithospheric mantle (see discussion in Section 5.3).

5.3. Nature and evolution of the sub-NE China SCLM

Mantle xenoliths in the Ordovician kimberlites from the eastern China indicate the thick, cool, and refractory Archean lithosphere. However, the Tertiary basalt-borne peridotite xenoliths reveal the presence of a thin, hot, and fertile lithosphere in the Cenozoic beneath eastern China [1,2,100]. It is generally accepted that the NCC is predominantly underlain by the juvenile and fertile lithospheric mantle, with few ancient and comparatively refractory lithospheric mantle relics in some places [10,18,26]. According to previous mantle xenolith studies globally, the $Mg^{\#}$ values of olivines are considered to be an indicator of the age of the SCLM [2,7]. The $Mg^{\#}$ values in olivine in clinopyroxene-poor lherzolites or refractory harzburgites are higher than 91 and are typically considered to be Archean–Proterozoic lithospheric mantle relics [101,102]. Conversely, fertile peridotite with olivines with $Mg^{\#}$ values lower than 90 is regarded as Phanerozoic lithospheric mantle that was more recently accreted [2,103]. In the present study, the Changbaishan and Longgang xenoliths possessed a broad range of Olivine-$Mg^{\#}$ values (86.9–91.3), which is characteristic of the mixture between Shangwang and Hebi (Fig. 1a). In Fig. S6 (online), the peridotite xenoliths mostly fall in the Phanerozoic field, with several also plotting in the Proterozoic field, and mainly follow the "oceanic" trend. The equilibrium temperatures of the Changbaishan and Longgang peridotite xenoliths are concentrated in the transitional zone between refractory and fertile peridotite without any obvious trend (Fig. S7 online). We thus suggest that there should be coexistence between the ancient refractory and fertile lithospheric mantle underneath the Changbaishan and Longgang area, which is consistent with previous studies [13,17,18]. This also corroborates our H_2O results in the studied peridotite.

Specifically, the studied peridotite xenoliths, with high H_2O contents in excess of 50 ppm (up to 132 ppm), might in fact represent newly accreted and cooled asthenospheric materials, while those with H_2O contents lower than 50 ppm (as little as 9 ppm) may represent thinned, relic ancient lithospheric mantle, which is consistent with study of the peridotite xenoliths from Cenozoic basalts in the NCC [91]. In summary, the lithospheric mantle beneath the Changbaishan and Longgang during the Late Cenozoic was predominated by a younger and more fertile lithospheric mantle with minor ancient and refractory keel. However, in previous studies, the direct mechanism of transformation of the lithospheric

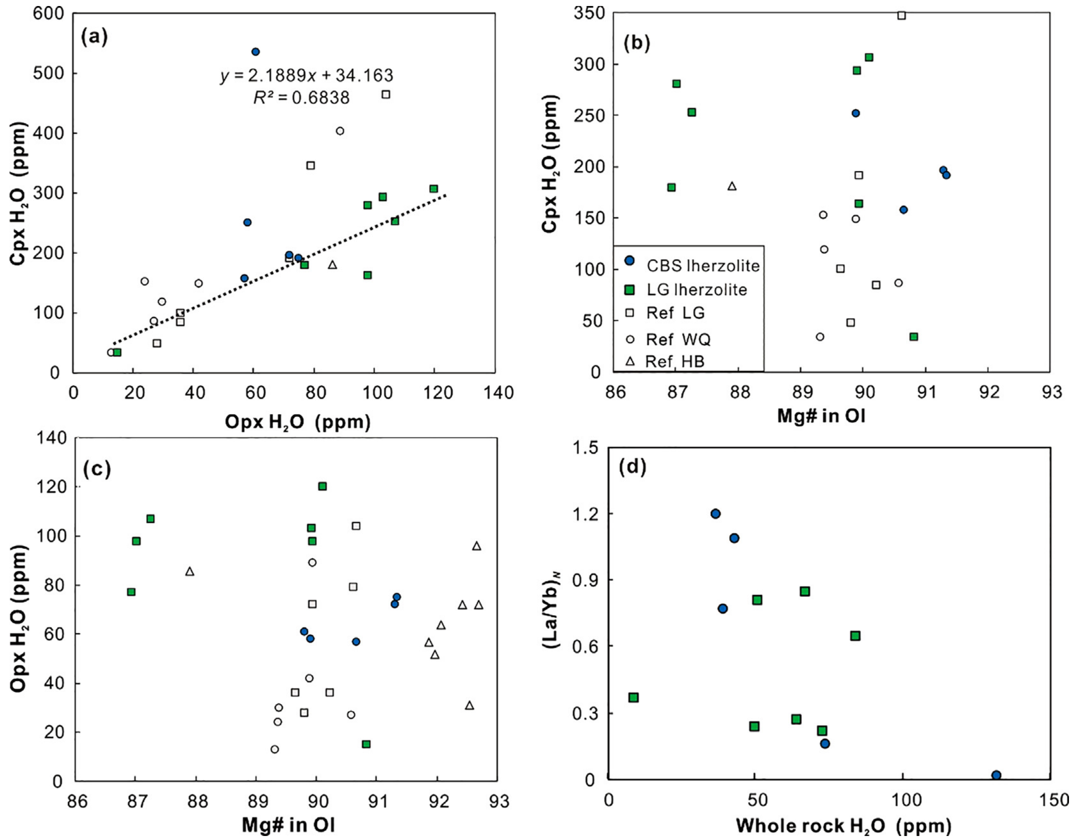

Fig. 6. The covariation of water contents in Cpx and Opx, and the relation of water contents with other geochemical signatures. (a) H_2O contents of clinopyroxene versus orthopyroxene, (b) H_2O contents of clinopyroxene versus $Mg^{\#}$ of olivine, (c) H_2O contents of orthopyroxene versus $Mg^{\#}$ in olivine, (d) $(La/Yb)_N$ versus whole-rock H_2O contents for the Changbaishan and Longgang peridotite. Ref refers to previous studies in studied area [91,98].

mantle of the studied area from ancient and refractory to younger and more fertile remains controversial, with models ranging from thermomechanical and chemical erosions [1,104], ancient crust delamination [100,105,106], and melt-peridotite reaction related to the subduction of the Pacific plate [15].

The mantle source beneath NE Japan might be affected by the fluids released from the subducting Pacific plate. For example, the mantle source for NE Japan basalts was strongly influenced by the fluids released from the subducting Pacific plate [107]. However, the area in the present study is far away from the Japan trench (1,000 km). Thus, the subduction-related fluids may have been lost before they could reach the mantle beneath NE China 1,000 km away from the trench [108]. Recent seismic tomography studies demonstrate that the Pacific slab has been dragged into the mantle transition zone beneath East Asia (ca. 410–660-km depth) [109–111]. In this review, deep stagnant subduction of the Pacific slab during the Late Cenozoic can be invoked as the dominant control on regional tectono-magmatism in NE Asia, such as the opening of the Japan Sea and the volcanism in NE China, as suggested by the abrupt reduction in the average convergence rate between the Eurasian and Pacific oceanic plates and subsequent slab rollback and trench retreat [112]. Under this extensional setting during the Late Cenozoic, a wet plume would ascend and transport previously recycled components (e.g., Pacific slab-derived materials oceanic crust and sediment) [111] into the upper mantle. These recycled components would act as metasomatic agents, which would interact with the above overriding ancient lithospheric mantle peridotite beneath NE China (Fig. S8 online). Thus, the ancient and refractory keel beneath NE China would be transformed into a fertile lithospheric mantle [13,17,18].

6. Conclusions

Integrated analyses of petrology, mineral chemistry, He-Ar isotopic compositions, and H_2O contents on mantle-derived xenoliths from the Changbaishan and Longgang regions of NE China led to the following general conclusions:

(1) The xenoliths are generally spinel-facies harzburgites and lherzolites for which the equilibration temperatures were between 863 and 1,141 °C. These should have undergone low to moderate fractional partial melting (1%–10%), followed by later fluid or hydrous silicate metasomatism.

(2) The results of He-Ar isotopes support that the peridotite xenoliths in both Changbaishan and Longgang were refertilized by melts/fluids from subduction-related oceanic materials.

(3) The H_2O contents of clinopyroxene and orthopyroxene ranged from 34 to 306 ppm and 15 to 120 ppm, respectively, and the high variation (9–132 ppm) in whole-rock H_2O might not be attributable to the variation in the degree of partial melting or mantle metasomatism, but might rather be an indication of their source character (newly accreted lithospheric mantle with a minor relic Archean lithospheric keel).

(4) The lithospheric mantle beneath Changbaishan and Longgang during the Late Cenozoic was predominantly substituted by a younger and more fertile lithospheric mantle with a minor ancient and refractory keel. Additionally, the westward-dipping Pacific oceanic plate subduction had an important influence on the lithospheric mantle of NE China.

Conflict of interest

The authors declare that they have no conflict of interest.

Acknowledgments

This work was supported by the Key Research Project of Frontier Sciences of Chinese Academy of Sciences (QYZDY-SSW-DQC030) and the National Natural Science Foundation of China (41476034). It also benefited from discussions with Drs. Ming Lei (Institute of Geology and Geophysics, Chinese Academy of Sciences, IGGCAS) and Wei Guo (IGGCAS). The authors appreciate the helpful input of the reviewers and editors.

Author contributions

Jiaqi Liu conceived and designed the research direction. Qinghu Xu wrote the paper, did the field work and collected samples; Huaiyu He and Yunhui Zhang performed the experiments and analyzed the data. All authors read and approved the final manuscript.

Appendix A. Supplementary data

Supplementary data to this article can be found online at https://doi.org/10.1016/j.scib.2019.07.006.

References

[1] Menzies MA, Fan W, Zhang M. Palaeozoic and Cenozoic lithoprobes and the loss of >120 km of Archean lithosphere, Sino-Korean Craton, China. Geol Soc Lond Spec Publ 1993;76:71–81.

[2] Griffin WL, O'Reilly SY, Ryan CG, et al. Secular variation in the composition of subcontinental lithospheric mantle: geophysical and geodynamic implications. Struct Evol Aus Continent 1998;26:1–26.

[3] Zheng JP, Griffin WL, Ma Q, et al. Accretion and reworking beneath the North China Craton. Lithosphere 2012;149:61–78.

[4] Xu YG, Zhang HH, Qiu HN, et al. Oceanic crust components in continental basalts from Shuangliao, Northeast China: derived from the mantle transition zone? Chem Geol 2012;328:168–84.

[5] Xu YG. Recycled oceanic crust in the source of 90–40 Ma basalts in North and Northeast China: evidence, provenance and significance. Geochim Cosmochim Acta 2014;143:49–67.

[6] Li HY, Xu YG, Ryan JG, et al. Olivine and melt inclusion chemical constraints on the source of intracontinental basalts from the eastern North China Craton: discrimination of contributions from the subducted Pacific slab. Geochim Cosmochim Acta 2016;178:1–19.

[7] O'Reilly S, Griffin WL, Djomani YHP, et al. Are Lithospheres forever? tracking changes in subcontinental lithospheric mantle through time. GSA Today 2001;11:4–10.

[8] Wu D, Liu Y, Chen C, et al. *In-situ* trace element and Sr isotopic compositions of mantle xenoliths constrain two-stage metasomatism beneath the northern North China Craton. Lithos 2017;288–289:338–51.

[9] Zhang H, Zheng JP, Pan SK, et al. Compositions and processes of lithospheric mantle beneath the west Cathaysia block, southeast China. Lithos 2017;286–287:241–51.

[10] Yang JH, Zhang M, Wu FY. Mesozoic decratonization of the North China Craton by lithospheric delamination: evidence from Sr-Nd-Hf-Os isotopes of mantle xenoliths of Cenozoic alkaline basalts in Yangyuan, Hebei Province, China. J Asian Earth Sci 2018;160:396–407.

[11] Wei Y, Mukasa SB, Zheng JP, et al. Phanerozoic lower crustal growth from heterogeneous mantle beneath the North China Craton: insights from the diverse Hannuoba pyroxenite xenoliths. Lithos 2019;324–325:55–67.

[12] Wan YS, Liu DY, Song B. An overview of the 2018 second class State Natural Science Award-North China Craton: formation and revolution of the oldest continent in China. Sci Bull 2019;64:641–3.

[13] Xu YG, Martin A, Matten F, et al. "Reactive" harzburgites from Huinan, NE China: products of the lithosphere-asthenosphere interaction during lithospheric thinning? Geochim Cosmochim Acta 2003;67:487–505.

[14] Chen Y, Zhang Y, Graham D, et al. Geochemistry of Cenozoic basalts and mantle xenoliths in Northeast China. Lithos 2007;96:108–26.

[15] Tang YJ, Zhang HF, Deloule E, et al. Slab-derived lithium isotopic signatures in mantle xenoliths from northeastern North China Craton. Lithos 2012;149:79–90.

[16] Wang J, Hattori K, Xie Z. Oxidation state of lithospheric mantle along the northeaster margin of the North China Craton: implications for geodynamic processes. Int Geol Rev 2013;55:1418–44.

[17] Lin AB, Zheng JP, Xiong Q, et al. A refined model for lithosphere evolution beneath the decratonized northeastern North China Craton. Contrib Mineral Petrol 2019;174:15.

[18] Park K, Choi SH, Cho M, et al. Evolution of the lithospheric mantle beneath Mt. Baekdu (Changbaishan): constraints from geochemical and Sr–Nd–Hf isotopic studies on peridotite xenoliths in trachybasalt. Lithos 2017;286–287:330–44.

[19] Liu DY, Nutman AP, Compston W, et al. Remnants of ≥3800 Ma crust in the Chinese part of the Sino-Korean craton. Geology 1992;20:339–42.

[20] Wilde SA, Zhao GC, Sun M. Development of the North China Craton during the late Archaean and its final amalgamation at 1.8 Ga: some speculations on its position within a global Palaeoproterozoic supercontinent. Gondwana Res 2002;5:85–94.

[21] Chen S, Li XP, Kong F, et al. Metamorphic evolution and zircon U-Pb ages of the nanshankou mafic high pressure granulites from the Jiaobei Terrane, North China Craton. J Earth Sci 2018;29:1219–35.

[22] Zhong Y, He C, Chen NS, et al. Tectonothermal records in migmatite-like rocks of the Guandi complex in Zhoukoudian, Beijing: implications for late neoarchean to proterozoic tectonics of the North China Craton. J Earth Sci 2018;29:1254–75.

[23] Sun W, Ding X, Hu YH, et al. The golden transformation of the Cretaceous plate subduction in the west Pacific. Earth Planet Sci Lett 2007;262:533–42.

[24] Dan W, Li XH, Wang Q, et al. Phanerozoic amalgamation of the Alxa Block and North China Craton: evidence from Paleozoic granitoids, U-Pb geochronology and Sr-Nd-Pb-Hf-O isotope geochemistry. Gondwana Res 2016;32:105–21.

[25] Zhang HF, Zou DY, Santosh M, et al. Phanerozoic orogeny triggers reactivation and exhumation in the northern part of the Archean-Paleoproterozoic North China Craton. Lithos 2016;261:46–54.

[26] Zhao Y, Zheng JP, Xiong Q, et al. Destruction of the North China Craton triggered by the Triassic Yangtze continental subduction/collision: a review. J Asian Earth Sci 2018;164:72–82.

[27] Hu S, Raza A, Min K, et al. Late Mesozoic and Cenozoic thermotectonic evolution along a transect from the North China Craton through the Qinling orogen into the Yangtze Craton, central, China. Tectonics 2006;25:TC6009.

[28] Li SZ, Suo YH, Santosh M, et al. Mesozoic to Cenozoic intracontinental deformation and dynamics of the North China Craton. Geol J 2013;48:543–60.

[29] Meng F, Gao S, Niu Y, et al. Mesozoic-Cenozoic mantle evolution beneath the North China Craton: a new perspective from Hf-Nd isotopes of basalts. Gondwana Res 2015;27:1574–85.

[30] Liu J, Chen NS, Su W. Tectonic boundary and ceasing time of amalgamation between the North China Craton and the North Qinling Belt. J Earth Sci 2018;29:1074–80.

[31] Wei H, Liu G, Gill J. Review of eruptive activity at Tianchi volcano, Changbaishan, northeast China: implications for possible future eruptions. Bull Volcanol 2013;75:706.

[32] Sun C, You H, Liu J, et al. Distribution, geochemistry and age of the Millennium eruptives of Changbaishan volcano, Northeast China – a review. Front Earth Sci 2014;8:216–30.

[33] Fan QC, Sui JL. Periods of Quarternary volcanic activity in Longgang area, Jilin Province. Acta Petrol Sin 2002;4:495–500 (in Chinese).

[34] Liu J. Study on geochronology of the Cenozoic volcanic rocks in northeast China. Acta Petrol Sin 1987:21–31 (in Chinese).

[35] He H, Zhu R, Saxton J. Noble gas isotopes in corundum and peridotite xenoliths from the eastern North China Craton: implication for comprehensive refertilization of lithospheric mantle. Phys Earth Planet Inter 2011;189:185–91.

[36] Kovács I, Hermann J, O'Neill HS, et al. Quantitative absorbance spectroscopy with unpolarized light: Part II. Experimental evaluation and development of a protocol for quantitative analysis of mineral IR spectra. Am Mineral 2008;93:765–78.

[37] Zheng JP, O'Reilly SY, Griffin WL, et al. Nature and evolution of Cenozoic lithospheric mantle beneath Shandong peninsula, Sino-Korean craton, eastern China. Int Geol Rev 1998;40:471–99.

[38] Zheng JP, O'Reilly SY, Griffin WL, et al. Relict refractory mantle beneath the eastern North China block: significance for lithosphere evolution. Lithos 2001;57:43–66.

[39] Sun SS, McDonough WF. Chemical and isotopic systematics of oceanic basalts: implications for mantle composition and processes. Geol Soc Lond Spec Publ 1989;42:313–45.

[40] McDonough WF, Sun SS. The composition of the Earth. Chem Geol 1995;120:223–53.

[41] Arai S. Characterization of spinel peridotites by olivine-spinel compositional relationships: review and interpretation. Chem Geol 1994;113:191–204.

[42] Pearce JA, Barker PF, Edwards SJ, et al. Geochemistry and tectonic significance of peridotites from the South Sandwich arc-basin system, South Atlantic. Contrib Mineral Petrol 2000;139:36–53.

[43] Ishii T, Robinson PT, Maekawa H, et al. Petrological studies of peridotites from diapiric serpentinite seamounts in the Izu-Ogasawara-Mariana Forearc, Leg 125. In: Fryer P, Pearce JA, Stokking LB, et al., (eds.), Proceedings of the Ocean Drilling Program, Scientific Results, Tokyo, Japan 1992; p. 445–486.

[44] Brey GP, Köhler T. Geothermobarometry in four-phase lherzolites II. New thermobarometers, and practical assessment of existing thermobarometers. J. Petrol 1990;31:1353–78.

[45] Wells PRA. Pyroxene thermometry in simple and complex systems. Contrib Mineral Petrol 1977;62:129–39.

[46] Sachtleben T, Seck HA. Chemical control of Al-solubility in orthopyroxene and its implications on pyroxene geothermometry. Contrib Mineral Petrol 1981;78:157–65.
[47] Nickel KG. Phase equilibria in the system SiO_2-MgO-Al_2O_3-CaO-Cr_2O_3 (SMACCR) and their bearing on spinel/garnet lherzolite relationships. Neues Jahrb Miner Abh 1986;155:259–87.
[48] Webb SAC, Wood BJ. Spinel-pyroxene-garnet relationships and their dependence on Cr/Al ratio. Contrib Mineral Petrol 1986;92:471–80.
[49] Hao YT, Xia QK, Liu S, et al. Recognizing juvenile and relict lithospheric mantle beneath the North China Craton: combined analysis of H_2O, major and trace elements and Sr-Nd isotope compositions of clinopyroxenes. Lithos 2012;149:136–45.
[50] Hao YT, Xia QK, Liu S, et al. Partial melting control of water contents in the Cenozoic lithospheric mantle of the Cathaysia block of South China. Chem Geol 2014;380:7–19.
[51] Hao YT, Xia QK, Jia ZB, et al. Regional heterogeneity in the water content of the Cenozoic lithospheric mantle of Eastern China. J Geophys Res Solid Earth 2016;121:517–37.
[52] Xia QK, Liu J, Liu SC, et al. High water content in Mesozoic primitive basalts of the North China Craton and implications on the destruction of cratonic mantle lithosphere. Earth Planet Sci Lett 2013;361:85–97.
[53] Asimow PD, Dixon JE, Langmuir CH. A hydrous melting and fractionation model for mid-ocean ridge basalts: application to the Mid-Atlantic Ridge near the Azores. Geochem Geophys Geosyst 2004;5:Q01E16.
[54] Dixon JE, Dixon TH, Bell DR, et al. Lateral variation in upper mantle viscosity: role of water. Earth Planet Sci Lett 2004;222:451–67.
[55] Simons K, Dixon J, Schilling JG, et al. Volatiles in basaltic glasses from the Easter-Salas y Gomez Seamount Chain and Easter Microplate: implications for geochemical cycling of volatile elements. Geochem Geophys Geosyst 2002;3:1–29.
[56] Workman RK, Hauri E, Hart SR, et al. Volatile and trace elements in basaltic glasses from Samoa: implications for water distribution in the mantle. Earth Planet Sci Lett 2006;241:932–51.
[57] Moreira M, Kunz J, Allègre C. Rare gas systematics in popping rock: isotopic and elemental compositions in the upper mantle. Science 1998;279:1178–81.
[58] Burnard P, Graham D, Turner G. Vesicle-specific noble gas analyses of "popping rock": implications for primordial noble gases in Earth. Science 1997;276:568–71.
[59] Matsumoto T, Honda M, McDougall I, et al. Noble gases in pyroxenites and metasomatised peridotites from the Newer Volcanics, southeastern Australia: implications for mantle metasomatism. Chem Geol 2000;168:49–73.
[60] Matsumoto T, Chen Y, Matsuda J. Concomitant occurrence of primordial and recycled noble gases in the Earth's mantle. Earth Planet Sci Lett 2001;185:35–47.
[61] Hellebrand E, Snow JE, Dick HJB, et al. Coupled major and trace elements as indicators of the extent of melting in mid-ocean-ridge peridotites. Nature 2001;410:677–81.
[62] Su BX, Zhou MF, Jing J, et al. Distinctive melt activity and chromite mineralization in Luobusa and Purang ophiolites, southern Tibet: constraints from trace element compositions of chromite and olivine. Sci Bull 2019;64:108–21.
[63] Norman MD. Melting and metasomatism in the continental lithosphere: laser ablation ICPMS analysis of minerals in spinel lherzolites from eastern Australia. Contrib Mineral Petrol 1998;130:240–55.
[64] Bhanot KK, Downes H, Petrone CM, et al. Textures in spinel peridotite mantle xenoliths using micro-CT scanning: examples from Canary Islands and France. Lithos 2017;276:90–102.
[65] Casagli A, Frezzotti ML, Peccerillo A, et al. (Garnet)-spinel peridotite xenoliths from Mega (Ethiopia): evidence for rejuvenation and dynamic thinning of the lithosphere beneath the southern Main Ethiopian Rift. Chem Geol 2017;455:231–48.
[66] O'Reilly SY, Griffin WL. Mantle metasomatism. In: Harlov DE, Austrheim H, editors. Metasomatism and the chemical transformation of rock: lecture notes in earth system sciences. Berlin: Springer; 2012. p. 467–528.
[67] Zangana NA, Downes H, Thirlwall MF, et al. Geochemical variation in peridotite xenoliths and their constituent clinopyroxenes from Ray Pic (French Massif Central): implications for the composition of the shallow lithospheric mantle. Chem Geol 1999;153:11–35.
[68] Stalder R, Foley SF, Brey GP, et al. Mineral-aqueous fluid partitioning of trace elements at 900–1200 °C and 3.0–5.7 GPa: new experimental data for garnet, clinopyroxene, and rutile, and implications for mantle metasomatis. Geochim Cosmochim Acta 1998;62:1781–801.
[69] Gregory MY, David HG, Vadin K. Carbonatite metasomatism in the Southeastern Australian lithosphere. J Petrol 1998;39:1917–30.
[70] Coltorti M, Bonadiman C, Hinton RW, et al. Carbonatite metasomatism of the oceanic upper mantle: evidence from clinopyroxenes and glasses in ultramafic xenoliths of Grande Comore, Indian Ocean. J Petrol 1999;40:133–65.
[71] Hilton DR, Hammerschmidt K, Teufel S, et al. Helium isotope characteristics of Andean geothermal fluids and lavas. Earth Planet Sci Lett 1993;120:265–82.
[72] Graham DW, Humphris SE, Jenkins WJ, et al. Helium isotope geochemistry of some volcanic rocks from Saint Helena. Earth Planet Sci Lett 1992;110:121–31.
[73] Su F, Xiao Y, He HY, et al. He and Ar isotope geochemistry of pyroxene megacrysts and mantle xenoliths in Cenozoic basalt from the Changle-Linqu area in western Shandong. Chin Sci Bull 2014;59:374–86 (in Chinese).
[74] Yamamoto J, Nishimura K, Sugimoto T, et al. Diffusive fractionation of noble gases in mantle with magma channels: origin of low He/Ar in mantle-derived rocks. Earth Planet Sci Lett 2009;280:167–74.
[75] Dunai TJ, Porcelli D. Storage and transport of noble gases in the subcontinental lithosphere. Rev Mineral Geochem 2002;47:371–409.
[76] Day JM, Barry PH, Hilton DR, et al. The helium flux from the continents and ubiquity of low-$^3He/^4He$ recycled crust and lithosphere. Geochim Cosmochim Acta 2015;153:116–33.
[77] Garapić G, Jackson MG, Hauri EH, et al. A radiogenic isotopic (He–Sr–Nd–Pb–Os) study of lavas from the Pitcairn hotspot: implications for the origin of EM-1 (enriched mantle 1). Lithos 2015;228–229:1–11.
[78] Chen H, Xia QK, Jannick I, et al. Nature and significance of the Early Cretaceous giant igneous event in eastern China. Earth Planet Sci Lett 2005;233:103–19.
[79] Chen H, Xia QK, Jannick I, et al. Changing recycled oceanic components in the mantle source of the Shuangliao Cenozoic basalts, NE China: new constraints from water content. Tectonophysics 2015;650:113–23.
[80] Xia QK, Liu J, István K, et al. Water in the upper mantle and deep crust of eastern China: concentration, distribution and implications. Natl Sci Rev 2019;6:125–44.
[81] Keppler H, Bolfan-Casanova N. Thermodynamics of water solubility and partitioning. Rev Mineral Geochem 2006;62:193–230.
[82] Mierdel K, Keppler H, Smyth JR, et al. Water solubility in aluminous orthopyroxene and the origin of Earth's asthenosphere. Science 2007;315:364–8.
[83] Yang X, Xia QK, Etienne D, et al. Water in minerals of the continental lithospheric mantle and overlying lower crust: a comparative study of peridotite and granulite xenoliths from the North China Craton. Chem Geol 2008;256:33–45.
[84] Woods SC, Mackwell S, Dyar D. Hydrogen in diopside: diffusion profiles. Am Mineral 2000;85:480–7.
[85] Stalder R, Skogby H. Hydrogen diffusion in natural and synthetic orthopyroxene. Phys Chem Miner 2003;30:12–9.
[86] Grant K, Ingrin J, Lorand JP, et al. Water partitioning between mantle minerals from peridotite xenoliths. Contrib Mineral Petr 2007;154:15–34.
[87] Peslier AH, Luhr JF, Post J. Low water contents in pyroxenes from spinel-peridotites of the oxidized, sub-arc mantle wedge. Earth Planet Sci Lett 2002;201:69–86.
[88] Gose J, Schmädicke E, Beran A. Water in enstatite from Mid-Atlantic Ridge peridotite: evidence for the water content of suboceanic mantle? Geology 2009;37:543–6.
[89] Xia QK, Hao YT, Li P, et al. Low water content of the Cenozoic lithospheric mantle beneath the eastern part of the North China Craton. J Geophys Res Solid Earth 2010;115:B07207.
[90] Kohlstedt DL, Mackwell SJ. Diffusion of hydrogen and intrinsic point defects in olivine. Z Phys Chem 1998;207:147–62.
[91] Demouchy S, Jacobsen SD, Gaillard F, et al. Rapid magma ascent recorded by water diffusion profiles in mantle olivine. Geology 2006;34:429–32.
[92] Peslier AH, Luhr JF. Hydrogen loss from olivines in mantle xenoliths from Simcoe (USA) and Mexico: mafic alkalic magma ascent rates and water budget of the subcontinental lithosphere. Earth Planet Sci Lett 2006;242:302–19.
[93] Tian ZZ, Liu J, Xia QK, et al. Water concentration profiles in natural mantle orthopyroxenes: a geochronometer for long annealing of xenoliths within magma. Geology 2017;45:87–90.
[94] Demouchy S, Bolfan-Casanova N. Distribution and transport of hydrogen in the lithospheric mantle: a review. Lithos 2016;240–243:402–25.
[95] Michael P. Regionally distinctive sources of depleted MORB: evidence from trace elements and H_2O. Earth Planet Sci Lett 1995;131:301–20.
[96] Hauri EH, Gaetani GA, Green TH. Partitioning of water during melting of the Earth's upper mantle at H_2O-undersaturated conditions. Earth Planet Sci Lett 2006;248:715–34.
[97] Roeder PL, Emslie R. Olivine-liquid equilibrium. Contrib Mineral Petrol 1970;29:275–89.
[98] Zhao Q, Xia QK, Liu S, et al. Water content and element geochemistry of peridotite xenoliths hosted by Cenozoic basalt in Longgang and Wangqing, Jilin Province. Earth Sci Front 2015;22:360–73.
[99] Hao YT, Xia QK, Tian ZZ, et al. Mantle metasomatism did not modify the initial H_2O content in peridotite xenoliths from the Tianchang basalts of eastern China. Lithos 2016;260:315–27.
[100] Gao S, Rudnick RL, Carlson RW, et al. Re-Os evidence for replacement of ancient mantle lithosphere beneath the North China Craton. Earth Planet Sci Lett 2002;198:307–22.
[101] Zheng JP, Griffin WL, O'Reilly SY, et al. Mechanism and timing of lithospheric modification and replacement beneath the eastern North China Craton: peridotitic xenoliths from the 100 Ma Fuxin basalts and a regional synthesis. Geochim Cosmochim Acta 2007;17:5203–25.
[102] Sun J, Liu CZ, Wu FY, et al. Metasomatic origin of clinopyroxene in Archean mantle xenoliths from Hebi, North China Craton: trace-element and Sr-isotope constraints. Chem Geol 2012;328:123–36.
[103] Xiao Y, Zhang HF, Fan WM, et al. Evolution of lithospheric mantle beneath the Tan-Lu fault zone, eastern North China Craton: evidence from petrology and geochemistry of peridotite xenoliths. Lithos 2010;117:229–46.
[104] Xu YG. Thermo-tectonic destruction of the Archaean lithospheric keel beneath the Sino-Korean Craton in China: evidence, timing and mechanism. Phys Chem Earth A Solid Earth Geodesy 2001;26:747–57.

[105] Gao S, Rudnick RL, Yuan HL, et al. Recycling lower continental crust in the North China Craton. Nature 2004;432:892–7.
[106] Gao S, Rudnick RL, Xu WL, et al. Recycling deep cratonic lithosphere and generation of intraplate magmatism in the North China Craton. Earth Planet Sci Lett 2008;270:41–53.
[107] Jun-ichi K, Takeyoshi Y. Contributions of slab fluid, matle wedge and crust to the origin of Quaternary lavas in the NE Japan arc. J Petrol 2006;47:2185–232.
[108] Zou H, Fan Q, Yao Y. U-Th systematics of dispersed young volcanoes in NE China: asthenosphere upwelling caused by piling up and upward thickening of stagnant Pacific slab. Chem Geol 2008;255:134–42.
[109] Huang JL, Zhao DP. High-resolution mantle tomography of China and surrounding regions. J Geophys Res 2006;111:B09305.
[110] Zhao DP, Tian Y, Lei JS, et al. Seismic image and origin of the Changbai intraplate volcano in East Asia: role of big mantle wedge above the stagnant Pacific slab. Phys Earth Planet Int 2009;173:197–206.
[111] Liu Z, Niu FL, Chen YJ, et al. Receiver function images of the mantle transition zone beneath NE China: new constraints on intraplate volcanism, deep subduction and their potential link. Earth Planet Sci Lett 2015;412:101–11.
[112] Northrup CJ, Royden LH, Burchfiel BC. Motion of the Pacific plate relative to Eurasia and its potential relation to Cenozoic extension along the eastern margin of Eurasia. Geology 1995;23:719–22.

Qinghu Xu is a Ph.D. candidate from the Institute of Geology and Geophysics, Chinese Academy of Sciences in 2019. Her research interest focuses on using noble gas isotopes and water contents to constrain the nature of lithospheric mantle in NE China.

Jiaqi Liu has been a professor from the Institute of Geology and Geophysics, Chinese Academy of Sciences (CAS) since 1999. His research interests include volcanic geology and volcanology, quaternary geology and environment.